Arabian Journal for Science and Engineering (2022) 47:13893–13905
https://doi.org/10.1007/s13369-022-06566-2

RESEARCH ARTICLE-ELECTRICAL ENGINEERING

Nonlinear Power System Stabilizer Design for Small Signal Stability Enhancement

Ibrahim M. Alotaibi[1] · Salim Ibrir[1] · Mohammad A. Abido[1,2,3] · Muhammad Khalid[1,2,3]

Received: 20 March 2021 / Accepted: 30 December 2021 / Published online: 29 January 2022
© King Fahd University of Petroleum & Minerals 2022

Abstract
The interconnected power system is exposed to a wide range of disturbances that may induce electromechanical oscillations of small magnitude and often persist for long periods. Such oscillations may sustain and grow, causing system separation if no adequate damping is provided. Conventional Power System Stabilizers (PSSs) are often used to provide the necessary damping torque to suppress the oscillation through the excitation system. The design of PSS in the previous work is either nonlinear or entirely linear based on a linearized model around an equilibrium point. Nonlinear controllers provide very robust performance. However, their complexity limits their deployment. On the other hand, linear-based PSSs are simple, but their performance degrades as the operating conditions move away from the region of attraction. Unlike previously published work, the design of the PSS in this paper explicitly uses the nonlinear model of the power system and linear control theory. This paper presents a nonlinear PSS based on feedback linearization. The Riccati equation is used to construct the new coordinate's linear controller. The efficacy of the presented study is demonstrated through a comparison with nonlinear-based and linear-based PSSs. Performing an in-depth analysis of inertia's impact on the system's stability concludes the proposed study.

Keywords Feedback linearization · Nonlinear control · Nonlinear power system stabilizers · Synergy control · Inertia reduction

List of Symbols

E_{FD}	Field voltage
$E_q^{'}$	Quadrature internal voltage
K_A	Exciter gain
i_d	Direct axis current [A]
i_q	Quadrature axis current
K_i	Linearizing constants $\forall i = \{1-6\}$
P_e	Electrical power in [MW]
P_m	Mechanical power [MW]
T_A	Exciter time constant
$T_{do}^{'}$	Transient time constant [s]
T_e	Electrical torque [N/m]
T_j	Time constants $\forall j = \{1-4\}$
U_{pss}	Power system stabilizer signal
V_R	Regulated voltage [Volt]
V_{ref}	Reference voltage
V_t	Terminal voltage
v_d	Direct axis voltage
v_q	Quadrature voltage
w_s	Synchronous speed [Rad/Sec]
$\dot{x}$	System dynamics $\forall \dot{x} \in \mathbb{R}^n$
x_d	Direct axis reactance
$x_d^{'}$	Transient reactance of the machine
$\dot{z}$	Dynamics in the new coordinate $\forall \dot{z} \in \mathbb{R}^n$
δ	Angular displacement of the rotor [Elec Rad /Sec]
ω	Actual rotor speed [rad/s]
ϕ	Suggested manifold
ζ	Damping ratio
ω_n	Undamped frequency [rad/s]
ω_d	Damped frequency [rad/s]

✉ Ibrahim M. Alotaibi
alotaibi.ib@gmail.com

[1] Electrical Engineering Department, King Fahd University of Petroleum and Minerals, Dhahran 31261, Saudi Arabia

[2] Researcher at K.A.CARE Energy Research and Innovation Center (ERIC), Dhahran 31261, Saudi Arabia

[3] Interdisciplinary Research Center in Renewable Energy and Power Systems (IRC-REPS), KFUPM, Dhahran 31261, Saudi Arabia

1 Introduction

Generally, power systems are inherently nonlinear and exhibit a wide range of transients during the operation, resulting in low-frequency oscillations and underdamped low-frequency speed that are complex to control. Currently, most generators have Automatic Voltage Regulators (AVRs) that negatively impact the power system's dynamic stability. The ultimate goal of AVR is to regulate the terminal voltage once it deviates from the reference voltage. AVR helps to maintain a reliable operation during steady-state operation conditions. However, the power system is also exposed to significant disturbances such as electrical faults, which reduce the terminal voltage, thereby affecting its ability to transfer a synchronizing power. In addition, poorly damped oscillations are undesirable in power systems due to their ability to alter the security and reliability of the network. Although the low frequency-oscillations are small in magnitude, they can decrease the machines' lifetime expectancy. Under such conditions, even with minor disturbances, if not taken care of, large generators may lose synchronism. Over the years, the methods to improve transient and small signal stability have evolved rapidly. However, their application needs to be carefully assessed. For instance, one or a combination of two methods can be applied to enhance the stability of any given system. High-speed fault clearing, reduction in transmission lines reactance, shunt compensation, dynamic braking, and Power System Stabilizers (PSS) are well-known methodologies to enhance power system stability. However, the fast excitation system supplemented with a PSS is the most economical and effective technique for suppressing low-frequency oscillations and improving overall stability [1]. Therefore, large-scale generators are equipped with Power System Stabilizers (PSS) to provide the damping through the supplementary excitation system. The basic principle of PSSs is to compensate for the phase lag caused by such disturbances.

A wide range of Power System Stabilizers has been proposed in the literature known as conventional PSSs. In the early days, fixed PSSs were used due to their simple structure and implementation. However, the power system undergoes different operating conditions and exhibits different characteristics, which requires a more sophisticated design to yield satisfactory results. Most of which are linear-based controllers that require linear approximation to the nonlinear system to be implemented. For instance, the proposed PSSs include, but are not limited to, classical-based controllers [2], optimal controllers [3], adaptive controllers [4], robust controllers [5–7], intelligent power system stabilizers [8–15], and limited research effort devoted to nonlinear controllers [16–21]. Although linear-based controllers have been widely used in the industry, the expectation to fail in providing satisfactory performance is relatively high due to the high nonlinearity of the power system. Therefore, it is essential to adapt nonlinear controllers that are robust and immunized against large deviations given different operation scenarios.

Feedback linearizing control is a nonlinear state feedback technique in which the complete set or some set of states are linearized using nonlinear feedback control and a suitable state coordinate transformation [22, 23]. Most feedback linearization techniques are either Input-to-State linearization or input–output linearization. In the former, the entire set of system states is linearized, whereas, in the latter, a complete linearization or a partial linearization can be achieved by careful selection of the new coordinate. The goal of the input–output linearization approach is to linearize the map between the actual output and the transformed input. While in input-to-state linearization, an artificial output is intelligently chosen to yield a total transformation where the relative degree matches the number of states. The relative degree refers to the total number required to differentiate the output until the control input appears in its expression. A linear controller can then be proposed to perform the required tasks. There are stringent conditions that should be met to have full-state linearization. Practically, input–output linearization is more common and can be sought for a large number of systems if they are minimum phase type. It is worthwhile to note that Input-to-State linearization coincides with input–output linearization if the resultant relative degree strictly matches the total number of state variables.

Synergetic control theory can be regarded as a new approach to solving nonlinear differential equations introduced by [24]. The synergetic algorithm maps the original set of differential equations to a new dynamical system in a way that it ensures the following: any trajectory in the state space ends in an attracting point; the attracting point is located at the solution of the original system; the rate at which the dynamical system approaches the attracting point is controllable [18, 25]. Generally, the author of [16, 17, 24] provides different methods for designing optimal controllers for dynamical systems, in which the coordination between the controllers and the expectation is sought. The synergetic control approach attempts to find an area of attraction for the new dynamical system with its conceived controllers [25]. Conceptually, creating an area of attraction or attractors characterizes the Synergetic Control Theory. Furthermore, the attractors are developed at the roots of the nonlinear differential equations. That is, this allows the proposed approach to converge rapidly.

An attractor can be points, contours, torus, or regions of fractal dimensionality. It is defined as the region in the dynamical system's state space that attracts all nearby trajectories. It may also represent the internal wishes of the dynamical system. Irrespective of the initial conditions, the system should move toward one of the attractors and remain there infinitely. If, for instance, the controllers fail to ful-

fill the system's requirements, the system becomes unstable. Stability analysis should then be carried out to identify such situations. Also, the system is considered unstable. If no attractors are present, the convergence in such cases is not permissible. Lyapunov stability theory can be applied to examine stability.

In this paper, the PSS is synthesized using three approaches: linear-based PSS, nonlinear feedback linearization-based PSS (FBL-based PSS), and nonlinear synergy control-based PSS. The linear-based controller uses a linear approximation of the dynamical system around the operating points. We propose a full-order nonlinear feedback linearization for the dynamical system in the presented paper. An exact linearization is performed using state transformation with nonlinear feedback control. A linear controller in the new coordinate is proposed to achieve the desired performance based on the Riccati equation's solution. The paper also addresses the impact of inertia reduction on the synchronous machine's angular displacement and velocity. An eigenvalue analysis is performed to quantify the effect of inertia on the system's stability. In the case of synergy control, a nonlinear controller is proposed to attract the system's trajectories into the suggested manifold. A comparative analysis is conducted on a typical single-machine-infinite-bus system (SMIB).

The rest of the paper is structured as follows: Sect. 2 reports the recent publications in the field. Section 3 formalizes the problem. The mathematical framework is developed in Sect. 4, while Sect. 5 discusses the solution methodology. The findings and the results obtained are delivered in Sect. 6. Highlighting the concluding remarks ends this study.

2 Related Work

Linear-based Power System Stabilizers have been widely deployed and proposed in the literature [7–15, 25–28]. For example, a robust Power System Stabilizer based on simulated annealing was proposed in [7]. The authors utilized a simulated annealing optimization technique to tune the parameters. The study showed a robust performance against different initial parameter settings. An eigenvalue analysis was also performed to investigate the feasibility of the proposed study. The tuning process of the PSS in [8–10] was inspired by the whale optimization algorithm. In [8], the PSS was tuned by minimizing a multi-objective function comprising the damping factor and damping ratio of lightly damped modes of the generators. The performance was tested on a standard benchmark consisting of thirty-nine buses and ten generators, while in [9], the authors used an eigenvalue-based objective function to tune the PSS. The proposed study was tested on a single-machine-infinite-bus and a multi-machine system with different operating conditions. Similarly, an enhanced version of the whale optimization algorithm for tuning the PSS was proposed in [10]. A reduced-order model was derived for the high order model of the system to minimize the Integral Square Error (ISE). The effectiveness of the proposed work was demonstrated and compared with renowned algorithms such as Particle Swarm Optimization (PSO), Differential Evolution (DE), and classical Whale Optimization Algorithm (WOA). In [11], the optimal design of the PSS was inspired by the BAT search algorithm based on the echolocation behavior of bats. The proposed BAT-based PSS's performance was demonstrated by a comparison with Genetic Algorithm-based PSSs and Conventional-based PSSs.

On the other hand, the authors of [26] and [27] used a fuzzy-based Power System Stabilizer to tune the parameters of the PSS in a typical power system layout. In [27], the proposed model was implemented on a single-machine-infinite-bus system. Moreover, the authors of [26] extended the work and applied a fuzzified-based PSS in a multimachine system. The proposed approach was validated through a simulation of a multimachine system. An indirect adaptive neural-based Power System Stabilizer was proposed in [29]. The proposed technique consisted of a neuro-controller used to generate a supplementary control signal to the excitation system, a neuro-identifier to model the power system dynamics, and adapts the neuro-controller parameters.

Limited research has been proposed in the area of nonlinear-based Power System Stabilizers [18–21, 29–31]. For instance, the authors of [17] presented a nonlinear PSS based on synergetic control theory. The design synthesis of the proposed PSS was based entirely on a simplified nonlinear model of the power system. The proposed model was implemented in a single-machine-infinite-bus system. The results showed superior performance when compared with Conventional-based PSS. A fuzzy-based sliding mode control to damp out the low-frequency oscillations was used in [19]. The adaptive low was derived using the Lyapunov stability theory, where the stability of the closed-loop system was guaranteed. The effectiveness of the proposed technique was tested in an area with an inter-area oscillation, while in [20] and [30], a second-order sliding mode control was proposed to offset an inter-area oscillation mode. Sliding Mode Control (SMC) has been known as a very powerful and robust control technique. However, SMC-based controllers suffer from chattering phenomena. Therefore, the authors of [20] have used second-order sliding mode (SOSMC) control to overcome SMC shortcomings. Similarly, SOSMC was used in [30] to damp out the low-frequency oscillations. The proposed method showed an outstanding performance against modeling uncertainties, which is not the case in conventional PSS. A typical IEEE 10 bus system and a 39-bus system were used to demonstrate the effectiveness of the proposed study. A sliding mode control using quadratic minimization

was also proposed in [32] for a single-machine-infinite-bus system. The method was validated and compared with the case of Linear-based PSS, whereas in [31], a nonlinear backstepping PSS was proposed to suppress the oscillations and improve the transient stability. The proposed controller was based on the fourth-order model of the synchronous machine. A three-machine power system model was used to demonstrate the effectiveness of the proposed technique.

The design of PSS in the previous work is either a nonlinear reduced-order model or entirely linear based on a linearized model around an equilibrium point. Nonlinear controllers provide very robust and outstanding performance. However, their complexity limits their deployment. On the other hand, linear-based PSSs are simple to implement, but their performance degrades as the operating conditions move away from the region of attraction. Unlike previously published work, the design of the PSS in this paper explicitly uses the nonlinear model of the power system and linear control theory. In that regard, the contribution of this paper can be summarized as follows:

- Designing a nonlinear Power System Stabilizer using Feedback Linearization considering full order model.
- Linearizing the dynamical system and providing a linear controller to stabilize the system.
- Implementing the nonlinear controller proposed by [24] and [18].
- Performing an extensive comparative analysis for the behavior of the system under different controller designs.
- Investigating the impact of inertia reduction on the trajectories of the system.

3 Problem Definition

In this paper, a simplified dynamic power system model known as a single-machine infinite bus power system (SMIB) is considered, as shown in Fig. 1, [7, 33, 34]. This system is composed of a synchronous generator that is driven by a turbine with a governor. The excitation system is controlled by an Automatic Voltage regulator (AVR) and a Power System Stabilizer (PSS). The single-axis dynamic model shown in Fig. 1 can be described by the following forth order model and a set of algebraic equations as provided in the sequel.

3.1 Power System Model

3.1.1 The swing equation

Describes the mechanical dynamics of the generator, which can be written as a set of first-order differential equations.

$$\dot{\omega} = \frac{\omega_s}{2H}[P_m - P_e - D(\omega - \omega_s)] \tag{1}$$

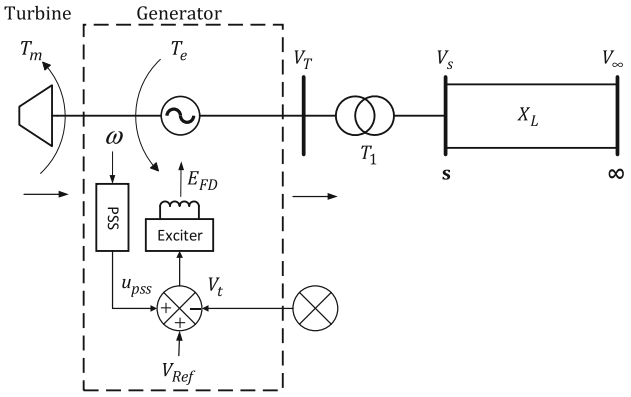

Fig. 1 Layout of a single-machine infinite-bus (SMIB) power system

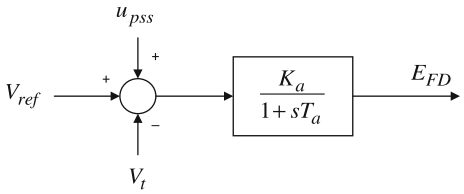

Fig. 2 IEEE type-1 simplified exciter

$$\dot{\delta} = \omega - \omega_s \tag{2}$$

δ is the angular displacement (i.e., rotor angle). P_e and P_m are the electrical power and mechanical power, respectively. ω and ω_s are the rotational speed and the synchronous speed, respectively. H is the inertia constant. D represents the damping coefficient.

3.1.2 Electrical dynamics of the generator

The mechanical power P_m is deemed constant throughout the analysis since the dynamics of the mechanical system are much slower than the dynamics of the electrical part. Therefore, the governor's action is not considered, and hence, it has no significant impact on the machine dynamics.

$$E\dot{q}' = \frac{1}{T'_{do}}\left[E_{FD} - Eq' - \left(x_d - x'_d\right)i_d\right] \tag{3}$$

3.1.3 Exciter dynamics

Equation (4) describes the internal dynamics of the simplified IEEE type 1 model shown in Fig. 2.

$$E_{FD} = \frac{1}{T_A}\left[K_A\left(V_{ref} - v_t + u_{pss}\right) - E_{FD}\right] \tag{4}$$

3.1.4 Algebraic equations

The following equations, which depend on the system states, are used to perform algebraic computations during the analysis.

$$T_e \triangleq P_e = \frac{E_q^{'} V_t}{x_d^{'}} \sin(\delta) \tag{5}$$

$$i_d = \frac{E_q^{'} - V_t \cos(\delta)}{x_d^{'}} \triangleq \frac{E_q^{'} - v_q}{x_d^{'}} \tag{6}$$

$$i_q = \frac{V_t \sin(\delta)}{x_q} \tag{7}$$

$$V_t = \sqrt{v_d^2 + v_q^2} \tag{8}$$

$$v_q = E_q^{'} - x_d^{'} i_d \tag{9}$$

$$v_d = i_q X_q \triangleq V_t \sin(\delta) \tag{10}$$

The dynamical equations of the generator can be written in the form $\dot{x} = f(x, u)$ as follows:

$$\begin{bmatrix} \dot{\delta} \\ \dot{\omega} \\ \dot{E}_q^{'} \\ \dot{E}_{FD} \end{bmatrix} = \begin{bmatrix} \omega - \omega_s \\ \frac{w_s}{2H}\left[P_m - \frac{E_q^{'} V_t}{x_d^{'}} \sin(\delta) - D(w - w_s)\right] \\ \frac{1}{T_{do}^{'}}\left[\left(E_{FD} - E_q^{'} - \frac{E_q^{'} - V_t \cos(\delta)}{x_d^{'}}\left(x_d - x_d^{'}\right)\right]\right. \\ \frac{1}{T_A}\left[K A\left(u_{pss} + V_{ref} - V_t\right) - E_{FD}\right] \end{bmatrix} \tag{11}$$

Writing the above system in the compact form $\dot{x} = f(x) + g(x)u$ yields:

$$\begin{bmatrix} \dot{x}_1 \\ \dot{x}_2 \\ \dot{x}_3 \\ \dot{x}_4 \end{bmatrix} = \begin{bmatrix} x_2 - \omega_s \\ \frac{\omega_s}{2H}\left[P_m - \frac{x_3 V_t}{x_d^{'}} \sin(x_1) - D(x_2 - \omega_s)\right] \\ \frac{1}{T_{do}^{'}}\left[\left(x_4 - x_3 - \frac{x_3 - V_t \cos(x_1)}{x_d^{'}}\left(x_d - x_d^{'}\right)\right]\right. \\ \frac{1}{T_A}\left[K A\left(V_{ref} - V_t\right) - x_4\right] \end{bmatrix} + \begin{bmatrix} 0 \\ 0 \\ 0 \\ \frac{K_A}{T_A} \end{bmatrix} u_{pss} \tag{12}$$

4 Mathematical Modeling

4.1 Linearized Model

Considering the third-order model of the machine, and the simplified IEEE type-1 exciter model as depicted in Fig. 2, the complete nonlinear model of the machine can be described by (13) through (16).

$$\dot{\omega} = \frac{\omega_s}{2H}\left[P_m - \frac{E_q^{'} V_t}{x_d^{'}} \sin(\delta) - D(\omega - \omega_s)\right] \tag{13}$$

$$\dot{\delta} = w - w_s \tag{14}$$

$$E\dot{q}^{'} = \frac{1}{T_{do}^{'}}\left[E_{FD} - Eq^{'} - \left(x_d - x_d^{'}\right) i_d\right] \tag{15}$$

$$E_{FD} = \frac{1}{T_A}\left[K_A\left(V_{ref} - v_t + u_{pss}\right) - E_{FD}\right] \tag{16}$$

Given the above nonlinear dynamical system and the algebraic equations given by (5) through (10), the linearization in terms of the initial conditions can be carried out as follows:

4.2 Derivation of the Linearization Constants

The complete derivation of the linearization process can be found in detail in [1, 23]. Linearizing around an operating point a and neglecting the higher-order terms, the electrical torque can be given by:

$$\Delta T_e = eq_0^{'} \times \Delta i_q + i_{q0} \Delta eq^{'} + \left(x_d - x_d^{'}\right)\left(i_{do} \Delta i_q + i_{qo} \Delta i_d\right) \tag{17}$$

$$\triangleq \Delta T_e \triangleq K_1 \Delta\delta + K_2 \Delta eq^{'}$$

where

$$\begin{bmatrix} K_1 \\ K_2 \end{bmatrix} = \begin{bmatrix} 0 \\ i_{qo} \end{bmatrix} + \begin{bmatrix} F_d & F_q \\ Y_d & Y_q \end{bmatrix} \begin{bmatrix} \left(x_q - x_d^{'}\right) i_{qo} \\ eq_0^{'} + \left(x_q - x_d^{'}\right) i_{do} \end{bmatrix} \tag{18}$$

F_d, F_q, Y_d and Y_q are provided in 'appendix'. Similarly, K_3 and K_4 can be derived from the field voltage (i.e., Eq. (17)). After the linearization and neglecting the higher-order terms, we have the following:

$$K_3 = \frac{1}{1 + \left(x_d - x_d^{'}\right) Y_d} \tag{19}$$

$$K_4 = \left(x_d - x_d^{'}\right) F_d \tag{20}$$

The terminal voltage of the machine has a major role in deriving the linearization constants K_5, K_6 which are described by (20) and (21).

$$\Delta v_t = K_5 \Delta\delta + K_6 \Delta eq^{'} \tag{21}$$

$$\begin{bmatrix} K_5 \\ K_6 \end{bmatrix} = \begin{bmatrix} 0 \\ \frac{V_{q0}}{v_{t0}} \end{bmatrix} + \begin{bmatrix} F_d & F_q \\ Y_d & Y_q \end{bmatrix} \begin{bmatrix} -\frac{x_d^{'} v_{q0}}{v_{to}} \\ x_q v_{do} / v_{to} \end{bmatrix} \tag{22}$$

4.3 Supplementary Excitation Control

The basic idea of the power system stabilizer is to apply a signal through the excitation system to increase the damping torque of the generator according to (23), as shown in Fig. 3. The PSS output signal is applied through the blocks that represent the electrical power of the synchronous machine

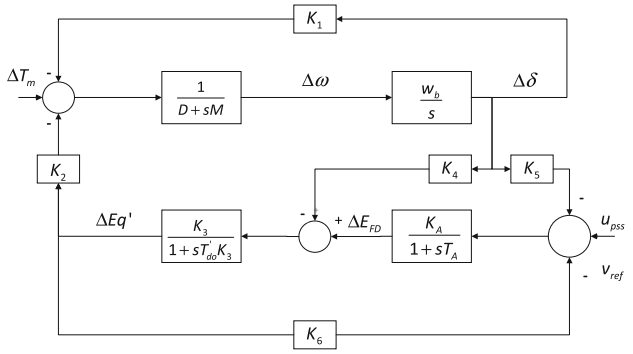

Fig. 3 Layout of SMIB

(i.e.,T_A, $T_{do}^{'}$ and K_2 blocks) to provide the necessary damping torque.

$$\dot{\Delta}\omega = (\Delta T_m - \Delta T_e - DT_d) \tag{23}$$

$$\Delta T_e = \Delta T_e + \Delta T_{e-new} = K_1\Delta\delta + D_E\Delta\omega \tag{24}$$

4.4 Power System Stabilizer Structure and Input Signals

A wide range of Power System Stabilizers has been proposed in the literature known as conventional controllers such as lead–lead PSS, proportional–integral–derivative controllers, and others that are sophisticated such as optimal, adaptive, and intelligent-based controllers. The most commonly used controller nowadays is the Lead–Lag Controller (CPSS). The input signals to the Power System Stabilizers may include one or a combination of the following:

- Speed deviation $\Delta\omega$
- Frequency deviation Δf
- Electrical power deviation ΔP_e
- Accelerating torque ΔP_a

4.4.1 Lead–Lag Power System Stabilizers

The Lead–Lag PSS may comprise one or multiple compensation blocks preceded by a washout block for resetting purposes, as shown below:

$$\begin{aligned} u_{pss} &= \frac{sT_w}{1+sT_w}\left(\frac{1+sT_1}{1+sT_2}\right)^p \times Y \\ u_{pss} &= \frac{sT_w}{1+sT_w}\left(\frac{1+sT_1}{1+sT_2}\right)\left(\frac{1+sT_3}{1+sT_4}\right) \times Y \end{aligned} \tag{25}$$

where Y denotes the input signal to the PSS.

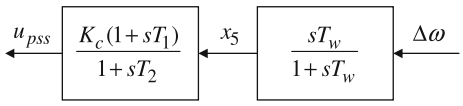

Fig. 4 Structure of Lead-Lag PSS

4.4.2 Proportional–Integral–Derivative (PID) Controller

$$u_{pss} = \frac{sT_w}{1+sT_w}\left(K_p + \frac{K_i}{s} + K_D s\right) \times Y \tag{26}$$

4.5 State Space Equations of Single-Machine-Infinite-Bus System

The state-space model of the single-machine-infinite-bus system can be derived from the block diagram provided in Fig. 3. In the standard form of first-order differential equations, the equivalent state-space model is as follows:

$$\begin{bmatrix} \Delta\dot{\delta} \\ \Delta\dot{\omega} \\ \Delta\dot{E}q^{'} \\ \Delta\dot{E}_{FD} \end{bmatrix} = \begin{bmatrix} 0 & w_b & 0 & 0 \\ -\frac{K_1}{M} & -\frac{D}{M} & -\frac{K_2}{M} & 0 \\ -\frac{K_4}{T_{do}^{'}} & 0 & -\frac{K_3}{T_{do}^{'}} & \frac{1}{T_{do}^{'}} \\ -\frac{K_A K_5}{T_A} & 0 & -\frac{K_A K_6}{T_A} & -\frac{1}{T_A} \end{bmatrix} \begin{bmatrix} \Delta\delta \\ \Delta\omega \\ \Delta Eq^{'} \\ \Delta E_{FD} \end{bmatrix} + \begin{bmatrix} 0 \\ 0 \\ 0 \\ \frac{K_A}{T_A} \end{bmatrix} u_{pss} \tag{27}$$

Equation (27) is in the compact form of $\dot{X} = Ax + Bu$. Where The state vector X is $\left[\Delta\delta; \Delta\omega; \Delta Eq'; \Delta E_{FD}\right]$. The open-loop eigenvalues of the system (26) can be obtained for $u_{pss} = 0$.

Considering the structure of the Lead-Lag PSS shown in Fig. 4 and augmenting the new states, namely the u_{pss} and x_5, we thus have the new closed-loop state matrix in the compact form:

$$\dot{Z} = A_c Z \tag{28}$$

A_c is the controlled system matrix having its closed-loop eigenvalues. It is clear that from the following matrix that the controller u_{pss} can stabilize the system.

$$\begin{bmatrix} \Delta\dot{\delta} \\ \Delta\dot{\omega} \\ \Delta\dot{E}q^{'} \\ \Delta\dot{E}_{FD} \\ \dot{x}_5 \\ \dot{u}_{pss} \end{bmatrix} = \begin{bmatrix} 0 & w_b & 0 & 0 & 0 & 0 \\ -\frac{K_1}{M} & -\frac{D}{M} & -\frac{K_2}{M} & 0 & 0 & 0 \\ -\frac{K_4}{T_{do}^{'}} & 0 & -\frac{K_3}{T_{do}^{'}} & \frac{1}{T_{do}^{'}} & 0 & 0 \\ -\frac{K_A K_5}{T_A} & 0 & -\frac{K_A K_6}{T_A} & -\frac{1}{T_A} & 0 & \frac{K_A}{T_A} \\ -\frac{K_1}{M} & -\frac{D}{M} & -\frac{K_2}{M} & 0 & -\frac{1}{T_w} & 0 \\ -K_1\lambda & -D\lambda & -K_2\lambda & 0 & \eta & -1/T_2 \end{bmatrix} \begin{bmatrix} \Delta\delta \\ \Delta\omega \\ \Delta Eq^{'} \\ \Delta E_{FD} \\ x_5 \\ u_{pss} \end{bmatrix} \tag{29}$$

where

$$\lambda \triangleq \frac{T_1 K_c}{T_2 M} \tag{30}$$

$$\eta \triangleq \frac{K_C}{T_2}\left(1-\frac{T_1}{T_w}\right) \tag{31}$$

or in compact form as:

$$\begin{bmatrix}\dot{x}_1\\ \dot{x}_2\\ \dot{x}_3\\ \dot{x}_4\\ \dot{x}_5\\ \dot{x}_6\end{bmatrix} = \begin{bmatrix} 0 & w_b & 0 & 0 & 0 & 0\\ -\frac{K_1}{M} & -\frac{D}{M} & -\frac{K_2}{M} & 0 & 0 & 0\\ -\frac{K_4}{T'_{do}} & 0 & -\frac{K_3}{T'_{do}} & \frac{1}{T'_{do}} & 0 & 0\\ -\frac{K_A K_5}{T_A} & 0 & -\frac{K_A K_6}{T_A} & -\frac{1}{T_A} & 0 & \frac{K_A}{T_A}\\ -\frac{K_1}{M} & -\frac{D}{M} & -\frac{K_2}{M} & 0 & -\frac{1}{T_w} & 0\\ -K_1\lambda & -D\lambda & -K_2\lambda & 0 & \eta & -1/T_2 \end{bmatrix}\begin{bmatrix}x_1\\ x_2\\ x_3\\ x_4\\ x_5\\ u_{pss}\end{bmatrix} \tag{32}$$

4.6 Nonlinear Control

4.6.1 Feedback Linearization

Feedback linearization is an efficient approach for nonlinear control design, which has attracted significant attention in recent years. The main idea is to algebraically transform the nonlinear dynamics into fully or partially linear systems, and thereby, linear control techniques can be proposed. Also, it is noteworthy that this approach precisely transforms the nonlinear system into a linear system, which is not the case in Jacobian linearization. Feedback linearization is achieved by exact state transformation to the system and a nonlinear controller that cancels the nonlinearity and injects a linear controller to stabilize the system. In input-state linearization, a new output is chosen, such that the relative degree of the system matches the number of states. By doing so, the Input-State Linearization coincides with the input–output linearization technique. The principle of such techniques is to differentiate the output until the control input u appears in the i^{th} derivative of y.

Consider the following system

$$\begin{aligned}\dot{x} &= f(x)+g(x)u\\ y &= h(x)\end{aligned} \tag{33}$$

where $\dot{x}$ is the state and u, y are the input and output of the system, respectively, which are both scalars.

$$\begin{aligned}\dot{y} &= \frac{\partial h}{\partial x}(f(x)+g(x)u)\\ \dot{y} &= L_f h(x)+L_g h(x)u\end{aligned} \tag{34}$$

where $L_f h(x)$ is the lie derivative of h along the vector field f (i.e., the dynamics of the given system). $L_g h$ represents the lie derivative of the h along the vector field g. Full linearization is permissible if the following holds true:

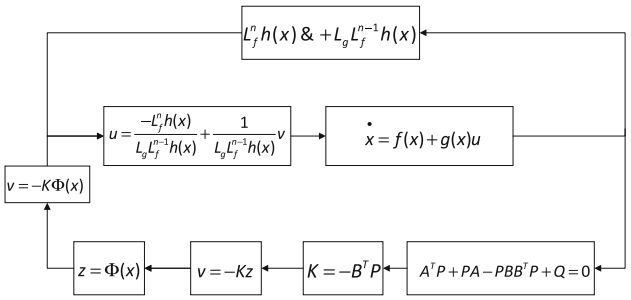

Fig. 5 Control layout using Feedback Linearization FBL

$$\begin{aligned}&y^n = L_f^n h(x)+L_g L_f^{n-1}h(x)u;\\ &L_g L_f^{n-1}h(x)u \neq 0\end{aligned} \tag{35}$$

y^n is the n^{th} derivative of the dynamical system of n states. The state transformation can be performed as follows:

$$z = \begin{bmatrix} h(x)\\ L_f h(x)\\ .\\ .\\ L_f^{n-1}h(x)\end{bmatrix} \tag{36}$$

$$\dot{z} = \begin{bmatrix} z_2\\ z_3\\ .\\ .\\ L_f^n h(x)+L_g L_f^{n-1}h(x)u\end{bmatrix} \tag{37}$$

The nonlinear controller is chosen as follows:

$$u = \frac{v}{L_g L_f^{n-1}h(x)} - \frac{L_f^n h(x)}{L_g L_f^{n-1}h(x)} \tag{38}$$

where v represents the linear controller in the form (39), which can be designed using any control architecture such as the Optimal Control, Pole Placement, and the solution to Riccati equation:

$$v = -K_1 z_1 - K_n z_n \tag{39}$$

The overall scheme of feedback linearization techniques is summarized in Fig. 5.

4.7 Synergetic Control

As pointed out in the preamble of the paper, the synergetic algorithm is somewhat motivated by the sliding mode control where a manifold or (i.e., a sliding surface) is suggested at

the roots of the dynamical system to attract all trajectories to operate along this manifold. Also, the manifold can be created based on the control objectives as a set of macrovariables ϕ_i that needs to be zeroed. The aggregated macrovariables are dependent on the state variables x_i and the control signals u_i(i.e., $\phi_i \triangleq \phi_i(x, u)$. The founder of this approach suggests the following constraint to be met with the surface $\phi_i = 0$.

$$T\dot{\phi} + \phi = 0 \tag{40}$$

where T is the time that determines the convergence to reach the manifold $\phi = 0$. The solution to the above differential equation is:

$$\phi(t) = \phi_0 e^{\frac{-t}{T}} \tag{41}$$

Obviously, global stability is guaranteed by the suggested differential equation. However, the surface should be well defined and designed to guarantee that $\phi = 0$. If we now consider $\dot{x} = f(x, u, t)$. Considering the chain rule of differentiation as follows:

$$\frac{d\phi(x,t)}{dt} \triangleq \frac{\partial\phi(x,t)}{\partial x}\frac{dx(t)}{dt} \tag{42}$$

If we plug the system dynamics and the suggested differential equation given by 39, we have:

$$\frac{T\partial\phi}{\partial x}\dot{x} + \phi = 0 \triangleq \frac{T\partial\phi}{\partial x} f(x, u, t) + \phi \tag{43}$$

Solving Eq. (40) for u yields:

$$u \triangleq \psi(x, t, \phi, T) \tag{44}$$

It is clear from the previous equation that the control input does not depend on the state variables only but also depends on the suggested manifold and the time T. Upon developing the controller, each surface introduces a new constraint on the system, and the designer can choose as many surfaces as control purposes. Throughout the development, it is clear that the synergetic approach operates on the natural nonlinear system without any linearization whatsoever. It is noteworthy that the synergized control law guarantees global stability on the surface. That is, once the trajectories are pulled into the surface, they are not supposed to leave the surface even if significant disturbances to the operating points take place.

5 Solution Methodology

5.1 Linearized Approach

The mathematical framework of the linearized approach has been extensively elaborated in the previous section, precisely in section A.

5.2 Nonlinear—Feedback Linearization Approach

Based on the introductory part elaborated earlier, along with the dynamical system described by (11), δ which is the rotor angle (i.e., the angular displacement) of the synchronous generator, has been selected as the new output in order to have a full linearization. The following development has been carried out using Maple, as provided in 'appendix'.

$$\begin{aligned} y_1 &= z_1 = x_1 = \delta \\ z_2 &= x_2 - w_s \\ z_3 &= \frac{w_s}{2H}\left\{P_m - \frac{x_3 V_\infty \sin(x1)}{X_T} - D(x_2 - ws)\right\} \\ z_4 &= -\frac{1}{2}\frac{w_s V_\infty x_3 \cos(x1)(x_2 - ws)}{2HX_T} - \gamma - \rho \end{aligned} \tag{45}$$

where γ and ρ and are as follows:

$$\gamma \triangleq \frac{w_s^2 D[P_m - x_3 V_\infty \sin(x_1)/X_T - D(x2 - w_s)]}{2H} \tag{46}$$

$$\rho \triangleq \frac{w_s V_\infty \sin(x1)}{2HX_T T_{do}}\left[x_4 - x_3 - \frac{x_3 - V_\infty \cos(x_1)\left(x_d - x_d^{'}\right)}{X_T}\right] \tag{47}$$

and $L_g L_f^{n-1} h(x)$ is given by (45):

$$L_g L_f^{n-1} h(x) = \frac{-w_s V_\infty \sin(x_1) K_A}{2 \times T_A T_{do} X_T H} \tag{48}$$

The dynamics in the new coordinate are:

$$\begin{bmatrix} \dot{z}_1 \\ \dot{z}_2 \\ \dot{z}_3 \\ \dot{z}_4 \end{bmatrix} = \begin{bmatrix} z_2 \\ z_3 \\ z_4 \\ L_f^n h(x) + L_g L_f^{n-1} h(x) u_{pss} \end{bmatrix} \tag{49}$$

$L_f^4 h(x)$ is provided in 'appendix'. The linear controller is suggested as the chain of integrators as follows:

$$\begin{aligned} v &= -K_1 z_1, \ldots - K_n z_n \\ z_1 &= \int_0^t \omega dt \end{aligned} \tag{50}$$

Furthermore, the controller gains are derived from the solution of the Riccati equation:

$$A^T P + PA - PBB^T P + Q = 0 \tag{51}$$

5.3 Nonlinear—Synergy Control Synthesis

The main goal of the PSS design is to stabilize the rotational speed through a controlling signal that is injected through the exciter. Therefore, the deviation in the rotor speed from the nominal value (i.e., 377 rad/s) is selected as a stabilizing signal on the surface. The deviation in the electrical power from the reference operating point is also added in the manifold. Defining the surface as:

$$\phi = k_1(\omega - \omega_{ref}) - (P_e - P_{ref}) \tag{52}$$

where $k_1 < 1$ is a positive coefficient. ω_{ref} and P_{ref} are the reference speed and reference power, respectively. The ultimate goal of the synergized controller is the force the trajectories of the system to operate on the surface $\phi = 0$. Using the previous development, we will develop the control law that derives the system along the manifold. Given the suggested ODE (50), and substituting (49) into (50), it yields (50)

$$T\dot{\phi} + \phi = 0 \tag{53}$$

$$K_1\dot{\omega} - P_e = -\frac{1}{T}\left[K_1(\omega - \omega_{ref}) - (P_e - P_{ref})\right] \tag{54}$$

$$P_e = \frac{V_\infty}{X_T}\sin(x_1)\dot{x}_3 + \frac{x_3 V_\infty \cos(x_1)}{X_T}\dot{x}_1 \tag{55}$$

where

$$\dot{x}_3 = \frac{1}{T_{do}}\left[K_e(x_4 + u_{pss}) - x_3 - \frac{x_3 - V_\infty\cos(x_1)\left(x_d - x_d^{'}\right)}{X_T}\right] \tag{56}$$

Solving for u_{pss} yields:

$$u_{pss} \triangleq \frac{1}{K_e}x_3 - x_4 + \frac{x_3 - V_\infty\cos(x_1)}{K_e X_T}\left(x_d - x_d^{'}\right) + \sigma + \beta \tag{57}$$

$$\sigma \triangleq -\Lambda X_T x_3 \cos(x_1)(\omega - \omega_s) + \frac{\Lambda K_1}{V_\infty \times 2H}[P_m - P_e - D(\omega - \omega_s)] \tag{58}$$

$$\beta \triangleq \frac{\Lambda}{V_\infty T_1}\left[K_1(\omega - \omega_{ref}) - (P_e - P_{ref})\right] \tag{59}$$

$$\Lambda \triangleq T_{do}X_T/K_e\sin(x_1) \tag{60}$$

5.4 Inertia reduction impact on the stability

This section addresses the impact of inertia variation on the behavior of the system due to the increased penetration of renewables. It has been pointed out that the large displacement of the conventional generating units results in a decreased inertia constant, which mainly affects the angular velocity of the committed machines (i.e., the frequency of the system) [35]. Such determinantal impact needs to be addressed. Therefore, we dedicate the following section to emphasize the impact of inertia variation on the trajectory of the system.

The state-space model shown in (29) is sufficient to investigate the system's performance near the equilibrium points for different values of H by conducting eigenvalue analysis. Using appropriate modal decomposition, (29) can be decomposed into a canonical form, which simplifies predicting the system's trajectories. However, such processes are beyond the proposed study's scope, and we shall limit ourselves to the model (29).

Once the dynamical system is linearized, the superposition technique can be applied to decouple the mechanical modes of the system as follows:

$$\frac{d^2\Delta\delta}{dt^2} + \frac{2\zeta\omega_n d\Delta\delta}{dt} + \omega_n^2\Delta\delta = 0 \tag{61}$$

The characteristic equation becomes:

$$s^2 + 2\zeta\omega_n + \omega_n^2 = 0 \tag{62}$$

which gives complex roots as:

$$\begin{aligned} s_{1,2} &= -\zeta\omega_n \pm j\omega_n\sqrt{1-\zeta^2} \\ \omega_n &= \sqrt{\left(\frac{\pi f P_{max}\cos(\delta_0)}{H}\right)} \\ \omega_d &= \omega_n\sqrt{1-\zeta^2} \\ \zeta &= \frac{D}{2}\sqrt{\frac{\pi f_0}{H P_{max}\cos(\delta_0)}} \end{aligned} \tag{63}$$

The trajectories of δ and ω due to a small perturbation in δ yield:

$$\begin{aligned} \delta &= \delta_0 + \frac{\Delta\delta_0}{\sqrt{1-\zeta^2}}e^{-\zeta\omega_n t}\sin(\omega_d t + \theta) \\ \theta &= \cos^{-1}(\zeta) \end{aligned} \tag{64}$$

$$\omega = \omega_0 - \frac{\omega_n\Delta\delta_0}{\sqrt{1-\zeta^2}}e^{-\zeta\omega_n t}\sin(\omega_d t) \tag{65}$$

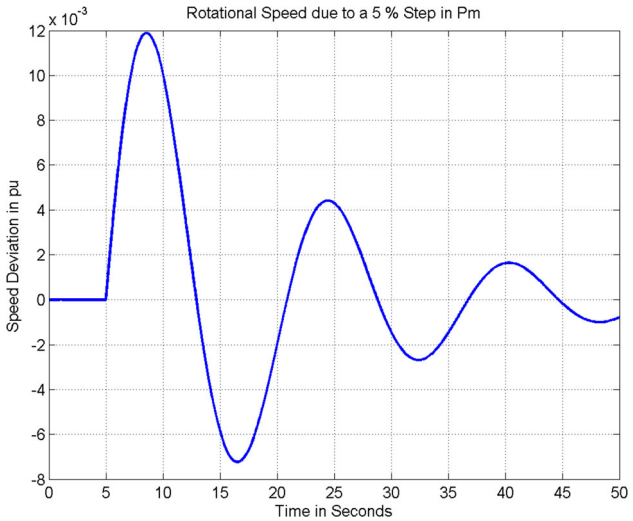

Fig. 6 Speed deviation due to a 0.05 step in P_m

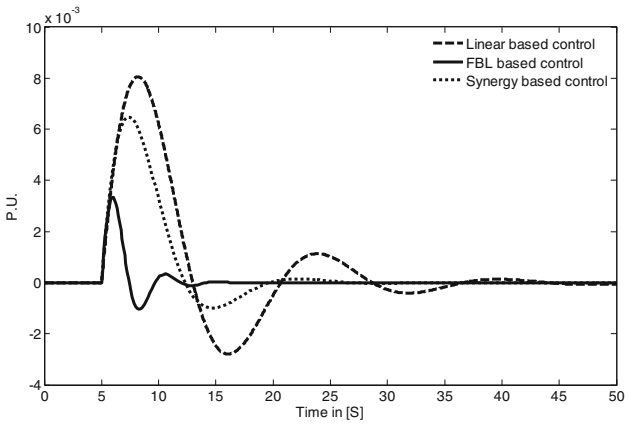

Fig. 7 Speed deviation under different scenarios

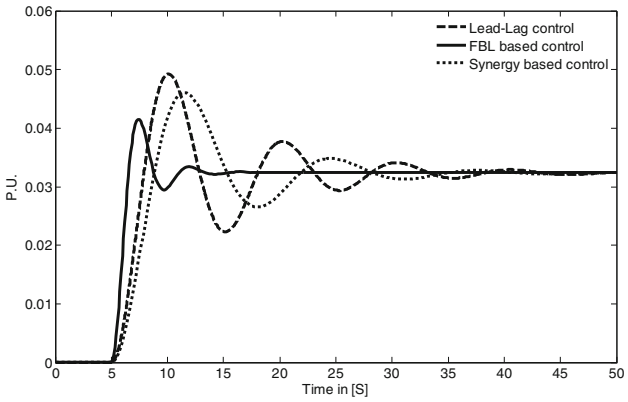

Fig. 8 Rotor angle behavior in different scenarios

6 Results and Discussion

6.1 Rotor Angle Stability Analysis

The following illustrative figures investigate the proposed nonlinear PSS performance for a step change in the mechanical power. Different control strategies were analyzed using the linear control approach, the proposed Feedback Linearization (FBL)-based PSS, and the nonlinear synergized PSS. Figure 6 depicts the rotor speed's behavior due to a disturbance with no control action taken whatsoever. It is clear that the oscillation lasted for a longer time but eventually settled to the nominal value.

Figure 7 shows the behavior of the speed once a step change in the mechanical power took place. The figure also shows the effectiveness of the proposed FBL controller in stabilizing the disturbance. It is expected for nonlinear PSSs to perform better than linear PSSs if the system experiences large disturbances. However, the proposed FBL-based PSS overcomes both nonlinear and linear PSS [12, 18], as depicted in Figs. 7 and 8. It is clear that the response of the speed under linear-based PSS [12] and nonlinear synergy-based PSS [18] suffered from long settling time and undesirable overshoot. On the other hand, the proposed FBL-based PSS successfully provided sufficient damping, which was clearly impacted on the level of overshoot and settling time.

The behavior of the rotor angle under different scenarios is depicted in Fig. 8. Clearly, the overshoot and the settling time under the FBL-based PSS structure were much smaller compared to the response of the system when using synergy-based PSS [18] and linear-based PSS [12]. Such reduction was also impacted on the rotor angular displacement, as shown in Fig. 8. The performance of the nonlinear controllers outperformed the linear controller design in all cases.

Figure 8 depicts the rotor angle response due to the disturbance under the FBL structure outperforming both the linear-based and the nonlinear synergic-based designs. The rotor angle under FBL was stabilized rapidly to a new operating point compared with linear and nonlinear synergetic-based controllers. The percentage of overshoot for the FBL-PSS and synergy-based PSS was reduced to 25% and 10%, respectively. Also, the settling time was much shorter in both cases compared with the conventional PSS. There was a significant reduction in the settling time for both cases, 51% and 37%, respectively. The system's response clearly shows that the overall performance under the FBL scheme is superior to both linear and nonlinear synergetic control structures.

Figure 9 shows the behavior of the manifold during the simulation. The manifold succeeded in attracting all the trajectories for the entire period once the disturbance took place at $t = 5s$.

Table 1 Impact of inertia variation on the eigenvalues of the system

State	$H = 9.26$	$H = 2$	$H = 4$	$H = 12$
δ	− 18.9648 + 0.0000i	− 25.2376 + 0.0000i	− 22.0106 + 0.0000i	− 17.7417 + 0.0000i
ω	− 5.2762 + 7.9481i	− 1.9434 + 13.3550i	− 3.6298 + 10.5460i	− 5.9514 + 6.9419i
E'_q	− 5.2762− 7.9481i	− 1.9434− 13.3550i	− 3.6298− 10.5460i	− 5.9514− 6.9419i
E_{fd}	− 0.8680 + 0.0000i	− 1.2443 + 0.0000i	− 1.1042 + 0.0000i	− 0.7475 + 0.0000i
$x_{washout}$	− 0.0164 + 0.1294i	− 0.0247 + 0.1416i	− 0.0219 + 0.1380i	− 0.0131 + 0.1227i
u_{pss}	− 0.0164− 0.1294i	− 0.0247− 0.1416i	− 0.0219− 0.1380i	− 0.0131− 0.1227i

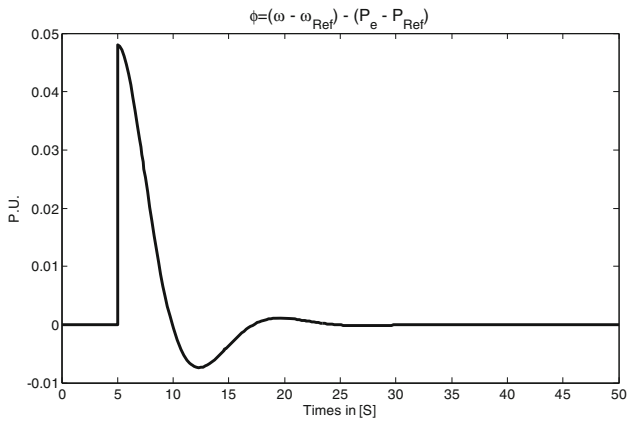

Fig. 9 Manifold behavior during the simulation under the synergized control scenario

6.2 The Impact of Inertia Reduction on System's Stability

6.2.1 Eigenvalues Analysis

This section investigates the performance of the dynamical system for different values of H. Table 1 summarizes the findings for different values of H. It is very clear that once the inertia constant is reduced, the amount of oscillations rapidly increases, which in turn affects the overall stability of the system. Furthermore, as the inertia increases, the real part of the eigenvalues moves away from the imaginary axis, allowing the system to sustain the disturbances more safely. Table 1 also shows that the variation in H is heavily impacted on the dynamics of the rotor's angular velocity ω.

6.2.2 *Rotor's Trajectories for Different Values of* H

Figures 10 and 11 show the behavior of the rotor dynamics for different values of H. Figure 10 shows that the more the H values the lesser is the minimum frequency after a disturbance. It is also noteworthy to point out that greater values of H shift the location of the minimum point, thus allowing more room for primary control action to take place.

On the other hand, the impact of H on the rotor angle is not direct. However, increasing the values of H results in a slightly more significant deviation and more settling time, as shown in Fig. 11.

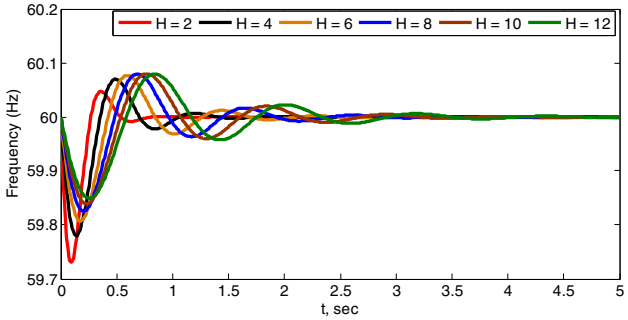

Fig. 10 Impact of different H values on the frequency

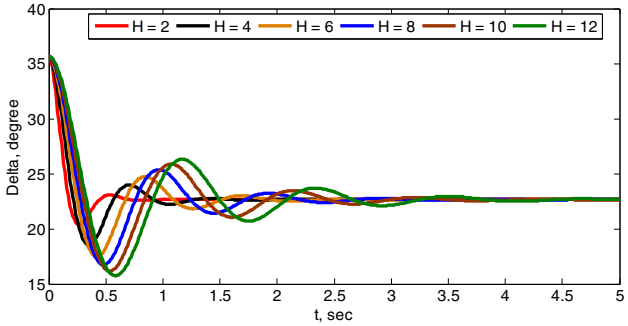

Fig. 11 Impact of different H values on the torque angle

7 Conclusion

This paper presented a PSS design for a single-machine-infinite-bus system using a feedback linearization algorithm. The synthesized FBL-based PSS overcomes the shortcomings of liner-based controllers by exploiting the exact model of the power system. The proposed methodology exploited the linear control theory to reconstruct the PSS. For achieving satisfactory performance, the parameters of the PSS were tuned based on the Riccati equation. The proposed control technique showed a robust and superior performance against unpredicted significant disturbances. Also, the controllers were insensitive to the variation in the operating conditions and the disturbance's size. The efficacy of the proposed

technique was demonstrated through a comparison with a nonlinear synergetic PSS and a conventional linear PSS. It is worth pointing out that the PSS synthesis for a multimachine system will be addressed in future work.

In addition, in the presented study, an in-depth analysis was carried out to investigate the impact of inertia on the system's response using eigenvalue analysis and the general solution of the dynamical system under a disturbance. The proposed study showed that different values of H play a vital role in determining the minimum frequency after the disturbances. It was also seen that the greater the values of H, the more room for the generators to maneuver during the disturbances (i.e., Primary control actions). The proposed study concluded that the impact of H on the rotor's angle was minimal. It, however, resulted in a longer settling time and higher overshoots.

Acknowledgements The authors would like to acknowledge the support provided by King Fahd University of Petroleum Minerals through Direct Fund project # DF201022. Mr. Alotaibi also acknowledges Electrical Engineering Department, Qassim University, Qassim 51411, Saudi Arabia. Dr. Abido also acknowledges the support provided by KACARE Energy Research & Innovation Center (ERIC), KFUPM.

Appendix

System Parameters

See Table 2.

Lie Derivative

$$Lf_4h = \mathcal{L}_1 + \mathcal{L}_2 + \mathcal{L}_3 + \mathcal{L}_4 + \mathcal{L}_5$$

where $\mathcal{L}_{i's}$ are defined as follows:

Table 2 System parameters used in the simulation

System Parameters			
δ_o	37.16	$Eq_o^{'}$	1.327
K_1	0.544	T_1	1.31
K_2	1.2	T_2	10
K_3	0.658	T_3	1.31
K_4	0.69	k_1	0.1
K_5	− 0.0955	T_{do}	4
K_6	0.822	K_a	50
T_a	0.01	K_e	1
T_w	5	H	4
P_m	1	X_T	0.8
D	4	$x_d^{'}$	0.6

$$\mathcal{L}_1 \triangleq \frac{\frac{1}{2}\omega_s x_3 V_\infty \sin(x_1)(x_2-\omega_o)}{Hx_d^{'}} + \frac{\frac{1}{4}\omega_s^2 x_3 D V_\infty \cos(x_1)}{H^2}$$

$$\mathcal{L}_2 \triangleq -\frac{\frac{1}{2}\omega_s V_\infty \cos(x_1)\left(x_4 - x_3 - \frac{(x_3 - V_\infty \cos(x_1))\left(x_d - x_d^{'}\right)}{x_d^{'}}\right)}{Hx_d^{'}T_{do}^{'}}$$

$$\mathcal{L}_3 \triangleq \frac{\frac{1}{2}\omega_s V_\infty^2 \sin^2(x_1)\left(x_d - x_d^{'}\right)}{Hx_d^{'2}T_{do}^{'}}(x_2-\omega_o)$$

$$\mathcal{L}_4 \triangleq \frac{1}{2H}\left[\frac{\frac{1}{2}\omega_s V_\infty \cos(x_1)(x_2-\omega_o)}{Hx_d^{'}} + \frac{\omega_s^2 D^2}{4}\right](P_m - P_e - D(x_2-\omega_o))$$
$$-\frac{\frac{1}{2}\omega_s V_\infty \cos(x_1)(x_2-\omega_o)}{Hx_d^{'}} + \frac{\frac{1}{4}\omega_s^2 D V_\infty \sin(x_1)}{H^2 x_d^{'}}$$
$$-\frac{\frac{1}{2}\omega_s V_\infty \sin(x_1)\left(-1 - \frac{x_d - x_d^{'}}{x_d^{'}}\right)}{Hx_d^{'}T_{do}^{'}}$$
$$\times \frac{x_4 - x_3 - \frac{(x_3 - V_\infty \cos(x_1))\left(x_d - x_d^{'}\right)}{x_d^{'}}}{T_{do}^{'}}$$

$$\mathcal{L}_5 \triangleq -\frac{\frac{1}{2}\omega_s V_\infty \sin(x_1)\left[K_A\left(V_{ref} - V_t\right) - x_4\right]}{Hx_d^{'}T_{do}^{'}T_A}$$

References

1. Kundur, P.: Power System Stability and Control. McGraw-Hill Education (1994)
2. Marić, P.; Kljajić, R.; Chamorro, H.R.; Glavaš, H.: Power system stabilizer tuning algorithm in a multimachine system based on s-domain and time domain system performance measures. Energies (2021). https://doi.org/10.3390/en14185644
3. Abd Elazim, S.M.; Ali, E.S.: Optimal power system stabilizers design via cuckoo search algorithm. Int. J. Electr. Power Energy Syst. **75**, 99–107 (2016). https://doi.org/10.1016/j.ijepes.2015.08.018
4. Hemmati, R.: Power system stabilizer design based on optimal model reference adaptive system. Ain Shams Eng. J. **9**(2), 311–318 (2018). https://doi.org/10.1016/j.asej.2016.03.002
5. Allaboyena, G. K., Yilmaz, M.: Robust power system stabilizer modeling and controller synthesis framework. In: 2019 IEEE International Conference on Electro Information Technology (EIT), May 2019, pp. 207–212. https://doi.org/10.1109/EIT.2019.8833656.
6. Singh, M.; Patel, R.N.; Neema, D.D.: Robust tuning of excitation controller for stability enhancement using multi-objective metaheuristic Firefly algorithm. Swarm Evol. Comput. **44**, 136–147 (2019). https://doi.org/10.1016/j.swevo.2018.01.010
7. Abido, M.A.: Robust design of multimachine power system stabilizers using simulated annealing. IEEE Trans. Energy Convers. **15**(3), 297–304 (2000). https://doi.org/10.1109/60.875496
8. Butti, D.; Mangipudi, S.K.; Rayapudi, S.R.: An improved whale optimization algorithm for the design of multi-machine power system stabilizer. Int. Trans. Electr. Energy Syst. **30**(5), e12314 (2020). https://doi.org/10.1002/2050-7038.12314

9. Dasu, B.; Mangipudi, S.; Rayapudi, S.: Small signal stability enhancement of a large scale power system using a bio-inspired whale optimization algorithm. Prot. Control Mod. Power Syst. **6**(1), 35 (2021). https://doi.org/10.1186/s41601-021-00215-w
10. Butti, D.; Mangipudi, S.K.; Rayapudi, S.: Model order reduction based power system stabilizer design using improved whale optimization algorithm. IETE J. Res. (2021). https://doi.org/10.1080/03772063.2021.1886875
11. Ali, E.S.: Optimization of power system stabilizers using BAT search algorithm. Int. J. Electr. Power Energy Syst. **61**, 683–690 (2014). https://doi.org/10.1016/j.ijepes.2014.04.007
12. Abd-Elazim, S.M.; Ali, E.S.: Power system stability enhancement via bacteria foraging optimization algorithm. Arab. J. Sci. Eng. **3**(38), 599–611 (2013). https://doi.org/10.1007/s13369-012-0423-y
13. Costa Filho, R.N.D.; Paucar, V.L.: A multi-objective optimization model for robust tuning of wide-area PSSs for enhancement and control of power system angular stability. Results Control Optim. **3**, 100011 (2021). https://doi.org/10.1016/j.rico.2021.100011
14. Li, M.; Chen, Y.: Designing of power system stabilizer based on neural-like P systems. Proc. Inst. Mech. Eng. Part J. Syst. Control Eng. **234**(2), 199–210 (2020). https://doi.org/10.1177/0959651819851668
15. Chaib, L.; Choucha, A.; Arif, S.; Zaini, H.G.; El-Fergany, A.; Ghoneim, S.S.M.: Robust design of power system stabilizers using improved harris hawk optimizer for interconnected power system. Sustainability (2021). https://doi.org/10.3390/su132111776
16. Kolesnikov, A.A.: The basis of the synergetic control theory. Ispo-Serv. (2002)
17. Kolesnikov, A.A.: Synergetic control theory. Energoatomizdat (1994)
18. Jiang, Z.: Design of a nonlinear power system stabilizer using synergetic control theory. Electr. Power Syst. Res. **79**(6), 855–862 (2009). https://doi.org/10.1016/j.epsr.2008.11.006
19. Farahani, M.; Ganjefar, S.: Intelligent power system stabilizer design using adaptive fuzzy sliding mode controller. Neurocomputing **226**, 135–144 (2017). https://doi.org/10.1016/j.neucom.2016.11.043
20. Tare, Arti. V., Jadhav, S. S., Pande, V. N., Ghanegaonkar, S. P.: Design of Power System Stabilizer as Second-Order Sliding Mode Controller. In: Smart Sensors Measurements and Instrumentation, pp. 295–305 Singapore, New York (2021). https://doi.org/10.1007/978-981-16-0336-5_24.
21. Verrelli, C.M.; Marino, R.; Tomei, P.; Damm, G.: Nonlinear robust coordinated PSS-AVR control for a synchronous generator connected to an infinite bus. IEEE Trans. Autom. Control. (2021). https://doi.org/10.1109/TAC.2021.3062174
22. Lu, Q.; Sun, Y.; Mei, S.: Nonlinear control systems and power system dynamics. Springer, US, Boston, MA (2001) https://doi.org/10.1007/978-1-4757-3312-9
23. Chernous'ko, F.L.; Ananievski, I.M.; Reshmin, S.A.: Control of nonlinear dynamical systems: methods and applications. Springer-Verlag, Berlin Heidelberg (2008) https://doi.org/10.1007/978-3-540-70784-4
24. Kolesnikov, A. A.: Introduction of synergetic control. In: 2014 American Control Conference, Jun. 2014, pp. 3013–3016. https://doi.org/10.1109/ACC.2014.6859397.
25. Bezuglov, A.: Synergetic control theory approach for solving systems of nonlinear equations (2005)
26. Bhattacharya, S.: Power system oscillation damping by intelligent power system stabilizer. In: 2016 IEEE 1st International Conference on Power Electronics, Intelligent Control and Energy Systems (ICPEICES), Jul. 2016, pp. 1–6. https://doi.org/10.1109/ICPEICES.2016.7853509.
27. Sreedivya, K. M., Jeyanthy, P. A., Devaraj, D.: Fuzzy logic based power system stabilizer for damping low frequency oscillations in power system. In: 2017 International Conference on Innovations in Electrical, Electronics, Instrumentation and Media Technology (ICEEIMT), Feb. 2017, pp. 201–205. https://doi.org/10.1109/ICIEEIMT.2017.8116835.
28. El-Metwally, K.A.; Hancock, G.C.; Malik, O.P.: Implementation of a fuzzy logic PSS using a micro-controller and experimental test results. IEEE Trans. Energy Convers. **11**(1), 91–96 (1996). https://doi.org/10.1109/60.486581
29. Liu, W.; Venayagamoorthy, G.K.; Wunsch, D.C.: Design of an adaptive neural network based power system stabilizer. Neural Netw. **16**(5), 891–898 (2003). https://doi.org/10.1016/S0893-6080(03)00129-1
30. Liao, K.; He, Z.; Xu, Y.; Chen, G.; Dong, Z.Y.; Wong, K.P.: A sliding mode based damping control of DFIG for interarea power oscillations. IEEE Trans. Sustain. Energy **8**(1), 258–267 (2017). https://doi.org/10.1109/TSTE.2016.2597306
31. Lee, S.-S., Li, S.-Y., Park, J.-K.: Nonlinear back-stepping controller design for the enhancement of transient stability in power systems. In: 2007 American Control Conference, Jul. 2007, pp. 5905–5910. https://doi.org/10.1109/ACC.2007.4282320.
32. Safie, S. I., Shah, M., Hasimah, A. R., Wahab, A., Yusri, H. M.: Sliding mode control power system stabilizer (PSS) for Single Machine Connected to Infinite Bus (SMIB). In: 2008 IEEE 2nd International Power and Energy Conference, Dec. 2008, pp. 122–126. https://doi.org/10.1109/PECON.2008.4762447.
33. Abido, M.A.: Optimal design of power-system stabilizers using particle swarm optimization. IEEE Trans. Energy Convers. **17**(3), 406–413 (2002). https://doi.org/10.1109/TEC.2002.801992
34. Yasaei, Y., Karimi-Ghartemani, M., Bakhshai, A., Parniani, M.: Design of a nonlinear power system stabilizer. In: 2010 IEEE International Symposium on Industrial Electronics, Jul. 2010, pp. 143–147. https://doi.org/10.1109/ISIE.2010.5637607.
35. Alotaibi, I.M.; Abido, M.A.; Khalid, M.: Primary frequency regulation by demand side response. Arab. J. Sci. Eng. (2021). https://doi.org/10.1007/s13369-021-05440-x